ENGINEERING RESEARCH JOURNAL (ERJ)
Vol. 1, No. 42 October 2019, pp.74-81.
Journal Homepage: www.feng.bu.edu.eg

4*4 Microstrip Patch Antenna Array used to Breast Cancer Detection System

Fatma A. Mostafa, Michael N. Mikhael and Hala A. Mansour

Faculty of Engineering at Shoubra, Benha University, Cairo, Egypt,

Abstract

Breast cancer is one of the most common diseases in the recent period, it is the second leading cause of death worldwide. More than 1.8 million new breast cancer cases are diagnosed every year worldwide. In Egypt, the estimated number of cancer cases According to the results of the national population-based cancer registration program increased in the period (20152020) from 19411 to 22682 and is expected to reach 46050 in 2050. In this paper, a system will be designed to detect breast cancer tumor. It consists of an array of 4*4 microstrip patch antenna operating at 8 GHz that transmit and receive signals from the breast. The scattering signals are collected by voltage network analyzer (VNA) that connected to pc to show the output image which illustrates if it is normal or malignant tissues.

Keywords: Microstrip Patch Antenna, Breast Cancer, Cancer Detection, CST Simulation, Microwave Imaging.

1. INTRODUCTION

Cancer, in general, is a type of disease that makes infected cells grow, change and multiply out of control. growth with the potential to spread into surrounding tissues and can affect any part of the body. Cancer is the second leading cause of death worldwide according to the American Cancer Society. In 2018 The International Agency for Research on Cancer (IARC) of the World Health Organization (WHO) has released an alarming report on its cancer incidence around the world, and predicted that the number of cancer cases in 2018 will rise to 18.1 million new cases and that the number of deaths from the disease will rise to 9.6 million [1]. Many women around the world are suffering from the spread of this disease, which causes many untreated problems due to lack of early diagnosis. Early diagnosis is an important reason to return life for many infected. There are numerous techniques for detection tumors [2] such that X-ray mammography, ultrasound, computed tomography (CT) and Magnetic Resonance Imaging (MRI) [3]. youthful ladies have some problems however these methods are not preferred because of ionizing radiation that causes cell death, damage within the body and gives false examination for patients with dense breast tissue [4]. In addition, ionization from mammograms has been shown to involve many health risks, which include the possibility of converting healthy tissue into malignancy. So, microwave imaging techniques (MWI) are developed for early diagnosis. MWI has many advantages [5][6] for example, cheaper, more protection (non-ionizing) and simpler accessibility. It is overcome the drawbacks in terms of false indication. The basis for microwaves to detect and locate the tumor is the distinction in the electrical properties of ordinary and harmful breast tissue [7]. The essential thought of utilizing a microwave imaging framework for breast disease location is to transmit electromagnetic waves from a transmitting antenna to the breast and get the dispersed waves at a receiving antenna. Differences between electric field and magnetic field for normal and malignant tissues are critical to recognize dangerous tissue's position and volume. The dielectric properties of malignant breast tissues are approximately ten times as large as normal breast tissues [8][9]. This is because malignant tissues contain much water and are more active than normal. In this manner, antenna choice assumes a significant job. There are several antenna types like horn, dipole, monopole, Yagi-antenna, etc. Microstrip antenna has more favorable advantages like small structure, cheap, lightness, low profile planar configuration and is easily manufactured.

There are several types of researches in the detection of breast cancer using different antennas: in 2018 [10], used wide-slot ultra-wideband antenna, the antenna operates at the range from 2.5 to 7 GHz, the detection depends on the dielectric properties of normal and malignant breast tissues at microwave frequencies.

In 2018 [11] also, used (5*5) array of coplanar waveguide fed (CPW-fed) microstrip antenna, operating at 6.12GHz.

In 2017 [12], used cylindrical wideband slotted patch antenna operates over the frequency range from 7.8 GHz up to 15 GHz. the cylindrical antenna has a high gain-bandwidth product to cover the frequency range from 7.5 GHz up to 18 GHz.

In 2016 [13], used a square patch microstrip antenna with three rectangular slots, operating at 13.27GHz.

In 2015 [14], used flexible of sixteen monopole antenna placed on the breast as an abra, operating at (2-4) GHz.

In 2015 [15] also, used microstrip patch antenna operating at 2.45GHz for breast cancer detection.

In 2012 [16] using a single layer microstrip antenna operating at 2.44GHz.

In this paper, the antenna structure is a rectangular Microstrip patch antenna operating at 8GHZ utilized with the end goal of microwave imaging over distinguishing carcinogenic tissue into breast structure and so, a simple 3D breast structure is displayed to characterize dangerous tissue. All simulations are calculated using the CST program. Double-Stage Delay Multiply and Sum Beamforming Algorithm (DMAS) used in the calculation of the output signal processing. Section 2 clarifies framework configuration, section 3 and 4 clarify simulation & results and conclusion, respectively.

2. System Design

In this section the whole system used in tumor breast detection as shown in Fig. (1) will explain.

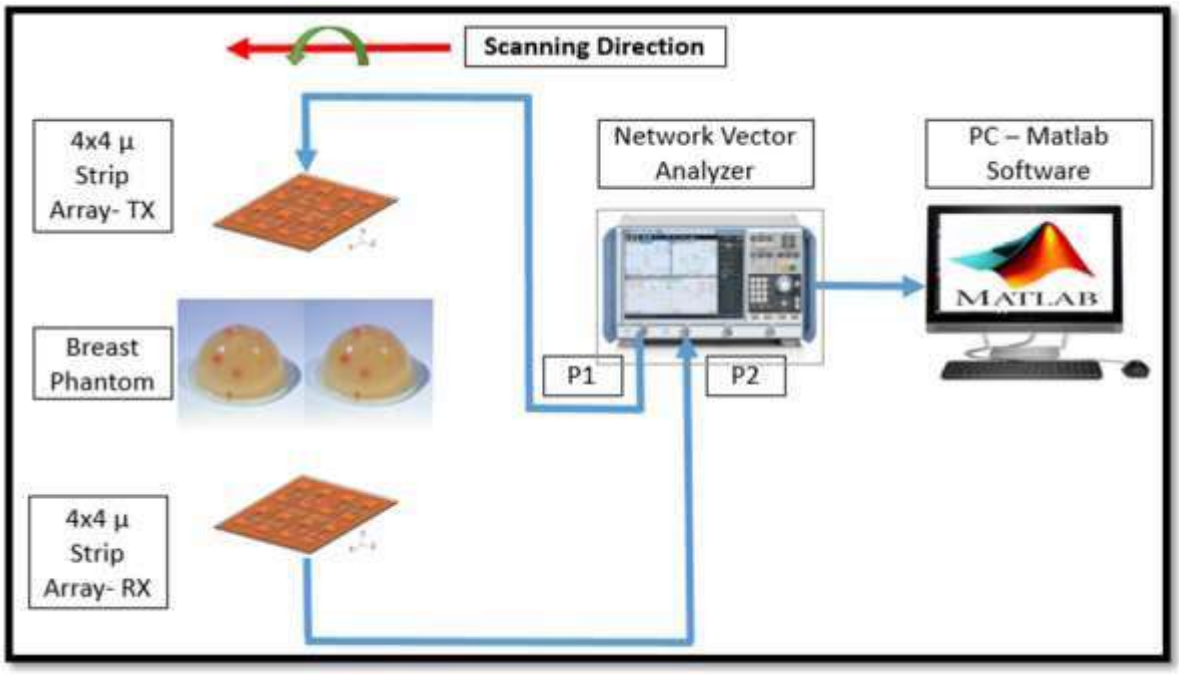

Fig. (1) Block diagram of the imaging system [17].

In the test room, we turn the phantom model to take information all around the phantom to recognize the situation of the tumor. The breast phantom is set between two antennas placed as they offset to each other and the effects of the breast tissues are studied on the performance of the antenna. The VNA parameters are set as IF bandwidth 10 HZ, 10 dBm output power, and 3.1 to 10.6 GHz frequency range. The transmitting antenna transmits the microwave pulse towards the breast phantom and the receiving antenna receives the dispersing signals reflected from the phantom. VNA collect the scattering signal from the receiving antenna and connect to PC to show the output image and recognize the output if it is normal tissues or malignant tissues (Image Processing). MATLAB is used to develop the fidelity equation and calculate its value by using Double-Stage Delay Multiply and Sum (DMAS) Algorithm.

2.1. Antenna Design

At first, our goals for antenna design are work on Wide range of frequency, Compatible penetration to human tissue, higher efficiency, and with high gain. So, used the band from 7GHZ to 9GHZ and used different substrate materials with different ε_r, and different substrate height to achieve our goals. calculating the Length of the Patch (L_p) and its Width (W_p) from the equations of rectangular microstrip patch antenna [18] as shown below: $Wp = \frac{C}{2f_0 * \sqrt{\frac{(\varepsilon_r+1)}{2}}}$. Eq. (1)

$$\varepsilon_{\bar{\bar{e}}ff} \frac{\varepsilon r+1}{2} + \frac{\varepsilon r-1}{2}\left[1+12\frac{h}{w}\right]^{-\frac{1}{2}}$$. Eq. (2)

$$L_{eff} = \frac{C}{2f_0\sqrt{\varepsilon_{eff}}}$$. Eq. (3)

$$\Delta L = 0.412h\frac{(\varepsilon_{eff}+0.3)(\frac{w}{h}+0.264)}{(\varepsilon_{eff}-0.258)(\frac{w}{h}+0.8)}$$

Eq. (4)

$$L_p = L_{eff} - 2\Delta L .$$

Eq. (5)

Inserting the results of W_p and L_p on CST simulator and run the program to give the Directivity, Bandwidth, and efficiency as shown in Table 1.

Table 1: illustrated the output results from CST simulator for one element of the antenna.

f(GHz)	h(mm)	Ɛr	W_p(mm)	L_p(mm)	Dir.(dBi)	BW(GHz)	η_{tot}(dB)	η_{rad}(dB)
7	1.5	4.4	13.03	9.633	7.125	0.3569	-3.434	-3.068
7	1.5	2.2	16.93	13.52	8.196	0.2631	-1.183	-0.3947
7	1.65	2.2	16.93	13.41	8.186	0.1673	-1.068	-0.3652
7	1.65	2.1	17.2	13.71	8.285	0.1131	-1.002	-0.3018
7.5	1.5	4.4	12.16	8.935	7.047	0.3413	-3.516	-3.054
7.5	1.5	2.2	15.8	12.54	8.217	0.2339	-1.177	-0.4218
7.5	1.65	2.2	15.8	12.43	8.206	0.2876	-1.094	-0.4311
7.5	1.65	2.1	16.05	12.71	8.312	0.216	-1.018	-0.3506
8	1.5	4.4	11.4	8.323	6.978	0.27181	-3.623	-3.076
8	1.5	2.2	14.81	11.69	8.235	0.3434	-1.173	-0.483
8	1.65	2.2	14.81	11.58	8.224	0.37025	-1.095	-0.4765
8	1.65	2.1	15.05	11.83	8.339	0.39709	-1.037	-0.3914
8.5	1.5	4.4	10.37	7.783	6.884	0.39843	-4.04	-3.186
8.5	1.5	2.2	13.94	10.93	8.268	0.41163	-1.188	-0.5375
8.5	1.65	2.2	13.94	10.82	8.255	0.44743	-1.13	-0.5376
8.5	1.65	2.1	14.16	11.06	8.376	0.46532	-1.068	-0.4564
9	1.5	4.4	10.14	7.301	6.897	0.4651	-4.859	-3.55
9	1.5	2.2	13.17	10.26	8.333	0.46532	-1.268	-0.5864
9	1.65	2.2	13.17	10.15	8.313	0.49217	-1.203	-0.5566
9	1.65	2.1	13.38	10.37	8.42	0.47427	-1.14	-0.5157

From the table results we used array of (4*4) microstrip patch antenna to improve overall gain with frequency range from 8GHZ to 9GHZ, substrate height 1.575 mm, and substrate material Rogers RT5880 with ε_r=2.2 F/m (available material in the National Research Center in Egypt). We made a comparison between a single element Fig. (2) and (4*4) array of rectangular microstrip patch antenna Fig. (3) to prove the improvement of gain. Substrate dimension L_s is 220 mm, W_s is 220 mm. Patch dimension W_p is 14.81 mm, L_p is 11.63mm. with the included SMA connector.

This substrate is financially accessible, minimal effort and simple to create the multilayer PCBs. A 50Ω SMA connector is used to feed the microstrip antenna. it has 2.08 dielectric permittivity and $4.62x10^4$ S/m electrical conductivity.

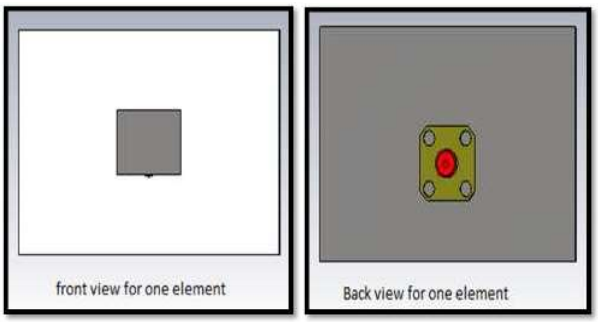

Fig. (2) single element structure.

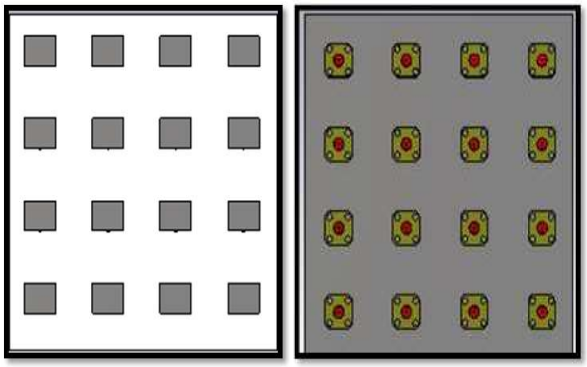

Fig. (3) front and back view for the (4*4) array antenna structure.

2.2. Breast Model

We don't have any human body or patient due to the safety permission, but we used Ultrasound-Guided Breast Biopsy Phantom shown in Fig. (4) that gives excellent image qualities and targets are colored to confirm successful sampling. Size: 136 mm diameter, 70 mm height, weight: 0.7 kg. We applied two economically accessible off-the-shelf homogeneous breast phantoms One is clear (ordinary tissues), and another is opaque with a single tumor of higher dielectric constant. The phantom is 160 x 80 mm2 size containing nearly standard dielectric properties as a human breast [19]. The Phantom comprises four layers. These are the skin layer, the breast tissue layer or fat, cancer malignant breast tumor and the ordinary air layer [20].

Fig. (4) Breast Model.

2.3. Vector Network Analyzer (VNA)

By using (R&S®ZNB20) VNA as shown in Fig. (5) that has a frequency range from 100 kHz to 20 GHz and the number of test ports 2 or 4 ports to test component specifications.it has versatile options such that time domain, eye diagram, mixer measurements, and more [21]. The antenna is connected to VNA to gather the dispersing signal. Connect the transmitted, received signals to the ports of VNA and connect the output to PC using the USB cable.

Fig. (5) ZNB20 VNA [22].

2.4. Image Processing

The frequency-domain data comes from VNA were preprocessed prior to imaging signal by MATLAB using DMAS algorithm. DMAS has high-quality images (higher contrast, lower side lobes, and higher resolution), and use in medical imaging [23]. In the DMAS calculation recreated picture features the electromagnetic dissipating instead of recuperating the dielectric profile [24] In the DMAS calculation recreated picture features the electromagnetic dissipating instead of recuperating the dielectric profile [24]. The frequency-domain information's were weighted with a differentiated Gaussian pulse and converted to time domain for the antenna using inverse discrete Fourier transform Eq. (6) [25].

$$y_{DMAS}(k) = \sum_{i=1}^{M-1} \sum_{j=i+1}^{M} x_{id}(k) x_{jd}(k)$$

Eq. (6)

6)where $x_{id}(k)$ and $x_{jd}(k)$ are the delayed detected signals for the i^{th} and j^{th} elements. The output image for signal previously recorded shown in Fig. (6).

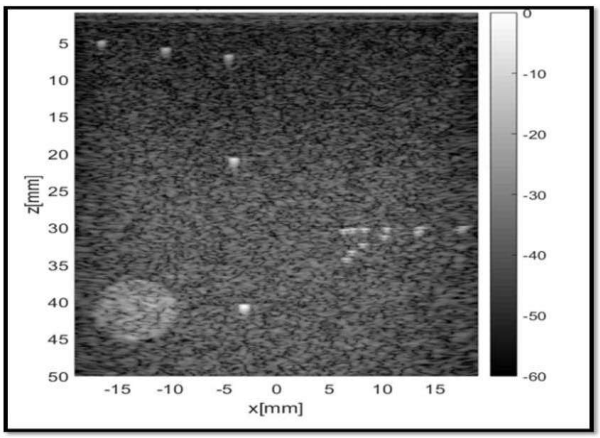

Fig. (6) DMAS image with a tumor.

3. Simulation and Results

The output radiation pattern from the array of (4*4) patch antenna at 8GHZ shown in Fig. (7).

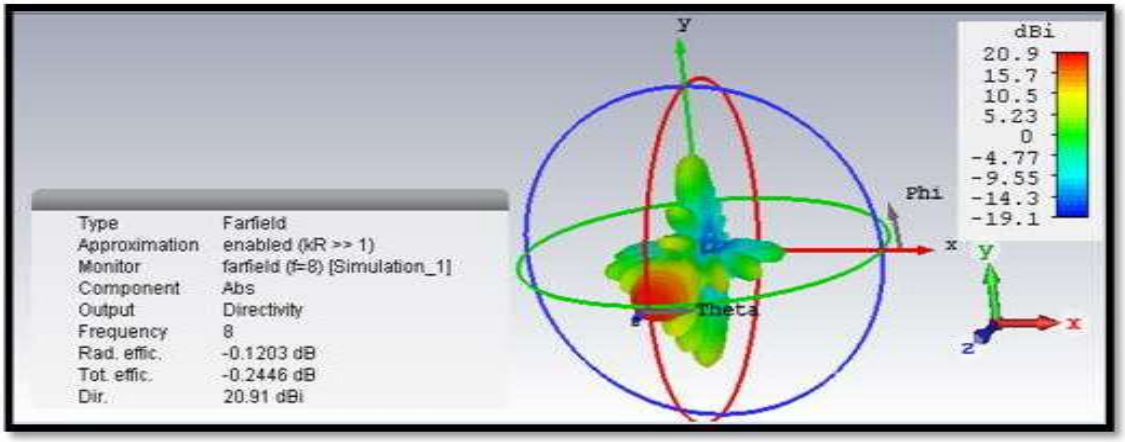

Fig. (7) radiation pattern output for the array from CST.

The S-Parameter for the Array shown in Fig. (8), the output Gain illustrated in Fig. (9), and the directivity curve shown in Fig. (10).

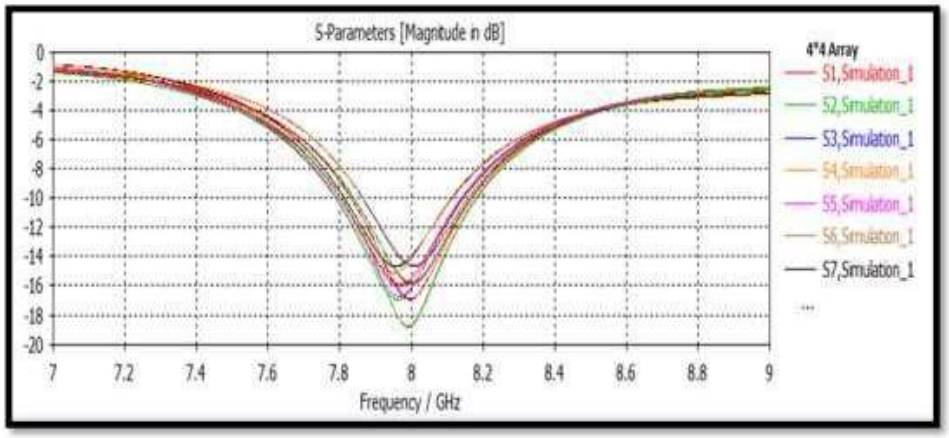

Fig. (8) S_{11}-Parameter output.

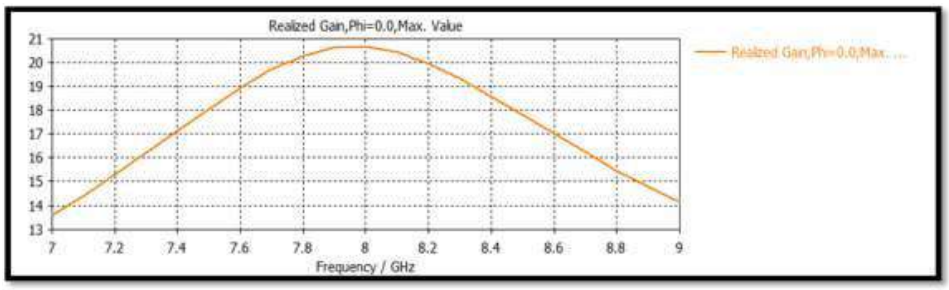

Fig. (9) output Gain for the array.

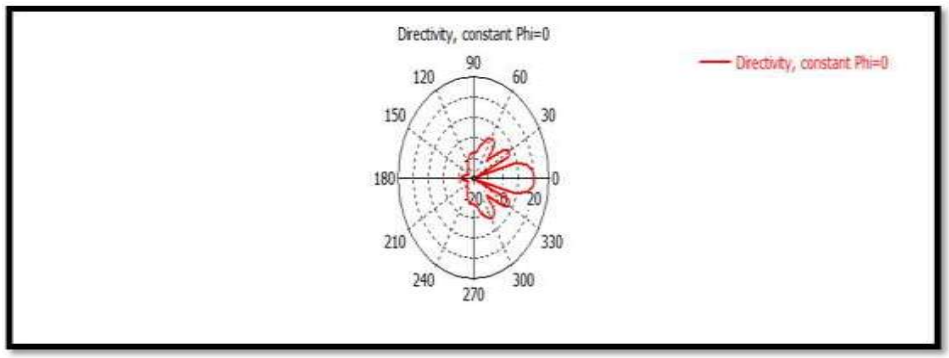

Fig. (10) Directivity curve for the array.

For single-element microstrip antenna output S-Parameter, Radiation Pattern, gain, Directivity simulation shown in Fig. (11), Fig. (12), Fig. (13), and Fig. (14) respectively.

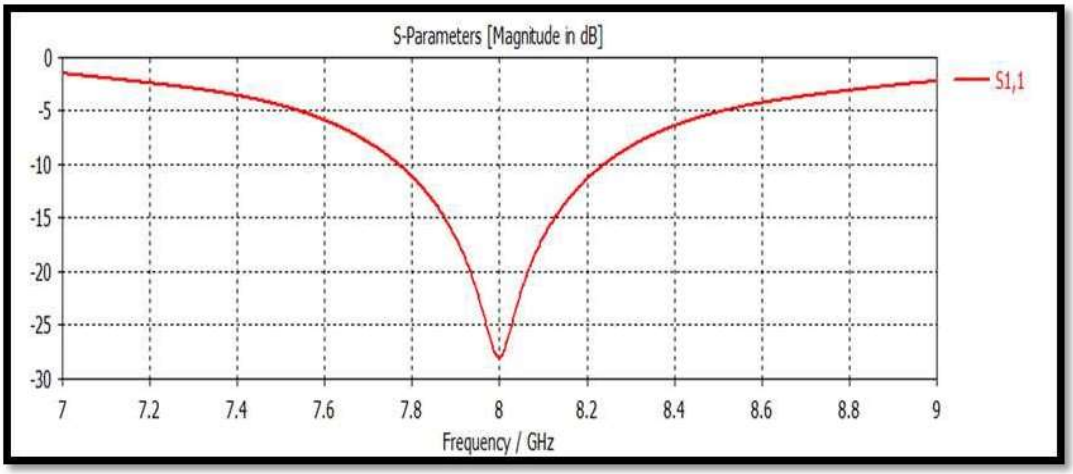

Fig. (11) S_{11}-Parameter for single element.

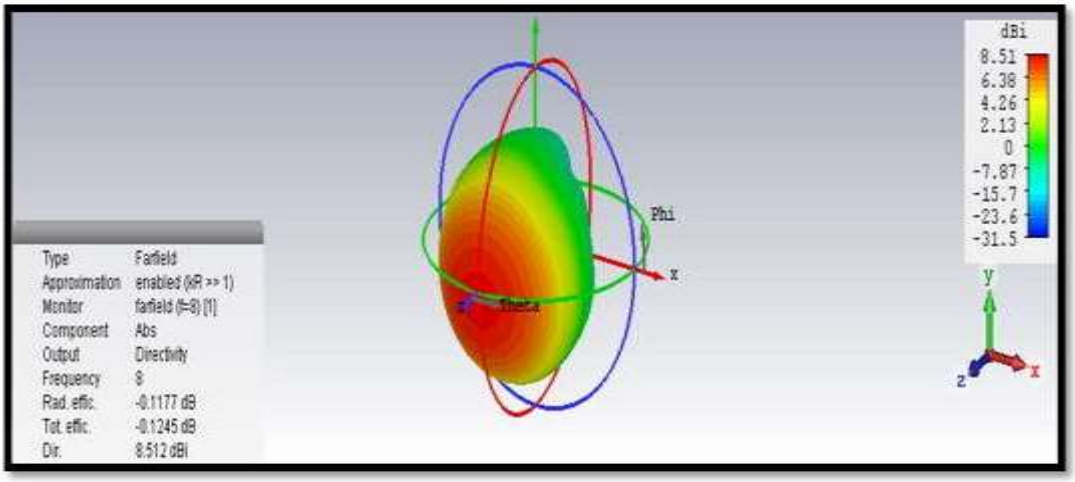

Fig. (12) Radiation pattern for single element.

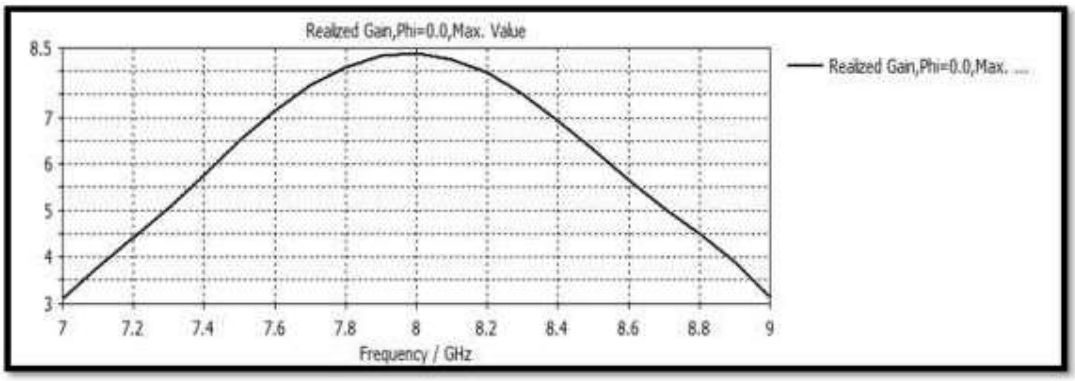

Fig. (13) the Gain curve for Single element.

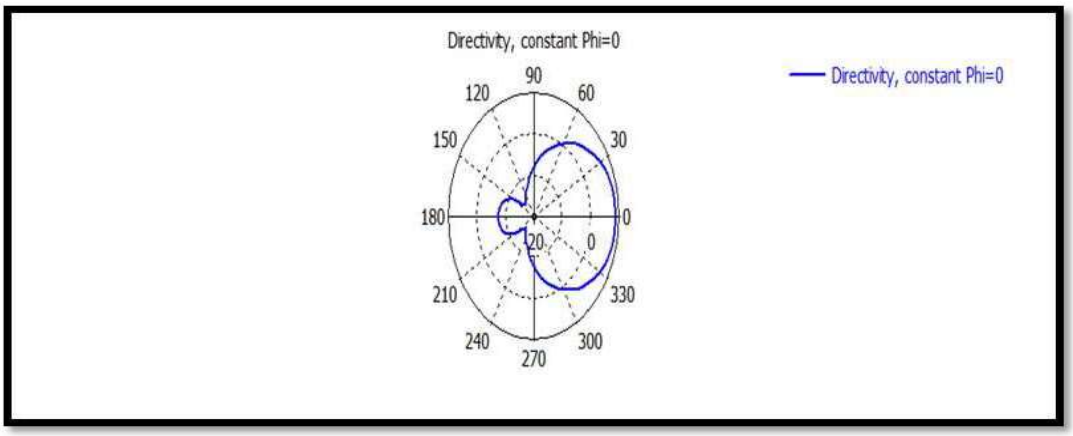

Fig. (14) Directivity curve for single element.

By making Comparison between Single element & (4*4) Array as shown in Fig. (13), and Fig. (14) for Gain and Total Efficiency respectively.

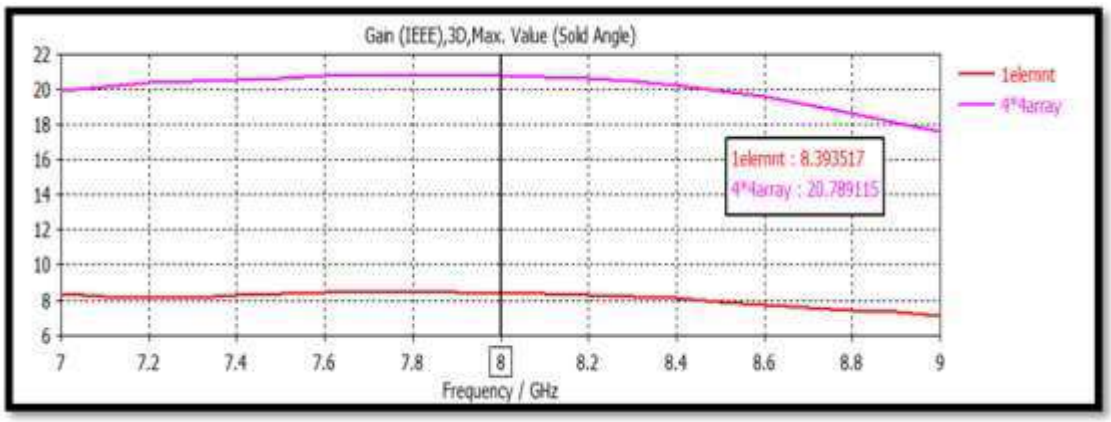

Fig. (13) Gain Comparison between Single element & (4*4) array.

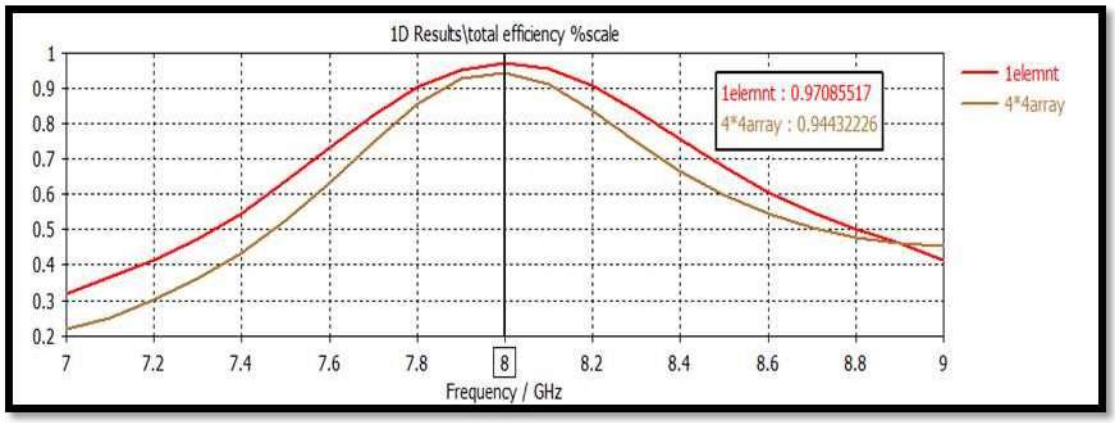

Fig. (14) Total Efficiency% scale Comparison between Single element& (4*4) array.

From the previous figures, we conclude that the total efficiency is closely in array& single element, the bandwidth increasing in the array than in Single element, gain, and Directivity is also increasing as shown in Table 2. So, an array of (4*4) Microstrip Patch Antenna has been used in our application to enhancement the gain and increasing BW.

Table 2: Comparison between Single element and (4*4) array.

Antenna output from CST	*Single element*	*Array of (4*4)*
Gain(8GHz)	**8.393517**	**20.789115**
% Efficiency	**0.97085517**	**0.94432226**
Directivity(dBi)	**8.512**	**20.91**

4. Conclusion

In this paper, the array of (4*4) rectangular microstrip patch antenna is studied to enhance gain and increasing bandwidth, operating at 8GHz.

substrate material is Rogers RT5880 (ε_r = 2.2 F/m).the maximum electric field = 34.138 $x10^3$ V/m, maximum magnetic field = 78.56 A/m and maximum current density distribution in breast = 20.76 A/m2 are evaluated by CST. The information's around the phantom, transmitter, receiver, and image processing program were recorded by MATLAB. The variety of dispersing signal because of the variety of dielectric properties of the phantom are analyzed and presented that determine if the tissues are ordinary or abnormal. The system has many advantages such as portable, cheap and easy installation. The system is tested with phantom breast prosthesis. Finally, the imaging system underpins the early discovery of breast tumor in the human breast.

5. References

[1] Geneva, Switzerland; "The International Agency for Research on Cancer (IARC)", sept2018.

[2] H. Zhang, ``Microwave imaging for ultra-wideband antenna based cancer detection," Ph.D. dissertation, School Eng., Univ. Edinburgh, Edinburgh, U.K., 2015.

[3] Wang L. (2017);" Early Diagnosis of Breast Cancer", Sensors,17(7),1572.

[4] C. K. Kuhl et al., ``Mammography, breast ultrasound, and magnetic resonance imaging for surveillance of women at high familial risk for breast cancer," J. Clin. Oncol., vol. 23, no. 33, pp. 84698476, 2005.

[5] A. Vispa, L. Sania, M. Paolia, A. Bigottia; meas.,146(2019)582.

[6] E.C. Fear, et al., "Enhancing breast tumor detection with near-field imaging," IEEE Microwave Mag., Vol. 3, pp. 48–56, 2002.

[7] Liewei Sha, Ward, E. R., & Stroy, B. (n.d.);SECON., sci- hub.tw/10.1109/.2002.995639.

[8] Kwon, S., & Lee, S. (2016); "Recent Advances in Microwave Imaging for Breast Cancer Detection, International Journal of Biomedical Imaging", scihub.tw/10.1155/2016/5054912.

[9] W. T. Joines, Y. Zhang, C. Li, and R. L. Jirtle, "The measured electrical properties of normal and malignant human tissues from 50 to 900 MHz," Med. Phys., vol. 21, no. 4, pp. 547_550, 1994.

[10] Gholipur, T., & Nakhkash, M. (2018). Optimized matching liquid with wide-slot antenna for microwave breast imaging. AEU - International Journal of Electronics and Communications, 85, 192–197.doi: 10.1016/j.aeue.2017.12.037.

[11] P.Chaudhary,A.Kumar;AEU.,107(2019)137.

[12] Ahmed I. Imran, Taha A. Elwi; JESTECH.,20(2017)990.

[13] A. Afyf, L. Bellarbi, N. Yaakoubi, E. Gaviot, L. Camberlein, M. Latrach, M.A. Sennouni; Procedia Eng., 168 (2016) 1334.

[14] H.Bahramiabarghouei, E. Porter , A.Santorelli ,B.Gosselin ,M. Popović ; IEEE T BIO-MED ENG.,62(2015)2516.

[15] R.Çalışkan,S.S.Gültekin, D.Uzer, Ö.Dündar;Procedia Soc Behav Sci.,195(2015)2905.

[16] Mahalakshmi, N., & Jeyakumar, V. (2012, July). Design and development of single layer Microstrip patch antenna for breast cancer detection.

[17] Z. MAHMUD, M. T. ISLAM, N. MISRAN, SAMSUZZAMAN;" Microwave Imaging for Breast Tumor Detection Using Uniplanar AMC based CPW-fed Microstrip Antenna", IEEE (2018).

[18] C. A. Balanis, Antenna Theory: Analysis and Design. Hoboken, NJ, USA: Wiley, 2016.

[19] M. Koutsoupidou et al., ``Evaluation of a tumor detection microwave system with a realistic breast phantom," Microw. Opt. Technol. Lett., vol. 59, no. 1, pp. 610, 2017.

[20] site [Online] Available at: https://www.erler-zimmer.de/shop/en/medicalsimulators/ultrasound/10157/ultrasound-guided-breast-biopsy-phantom-set-of-one-basicand-one-advanced-breast.

[21] data sheet[Online] Available at: https://scdn.rohdeschwarz.com/ur/pws/dl_downloads/dl_common_library/dl_brochures_and_datasheets/pdf_1/service_support_30/ZNB_dat-sw_en_5214-5384-22_v0900_96dp.pdf.

[22] product details [Online]for shopping: https://www.testwall.com/product/rohdeschwarzznb20-2/.

[23] Mozaffarzadeh M, Mahloojifar A, Orooji M, Adabi S, Nasiriavanaki M. Double stage delay multiply and sum beamforming algorithm: Application to linear-array photoacoustic imaging. IEEE Transactions on Biomedical Engineering, 2017e.

[24] M. Mozaffarzadeh, M. Orooji, A. Mahloojifar, M. Sadeghi (2018);" Double-Stage Delay Multiply and Sum Beamforming Algorithm Applied to Ultrasound Medical Imaging", Ultrasound in Medicine & Biology,44(3), p677-686.

[25] Yang M, Sampson R, Wei S, Wenisch TF, Chakrabarti C. Separable beamforming for 3-d medical ultrasound imaging. IEEE Transactions on Signal Processing, 2015;63:279–290.